Available online at www.sciencedirect.com
ScienceDirect
Journal of the European Ceramic Society 29 (2009) 2119–2128
www.elsevier.com/locate/jeurceramsoc

Temperature dependent hardness and strength properties of TiB_2 with $TiSi_2$ sinter-aid

G.B. Raju [a,*], B. Basu [a], N.H. Tak [b], S.J. Cho [b]

[a] *Laboratory for Advanced Ceramics, Department of Materials and Metallurgical Engineering, Indian Institute of Technology, IIT-Kanpur 208016, India*
[b] *Advanced Industrial Technology Group, Korea Research Institute of Standards and Science, Republic of Korea*

Received 12 August 2008; received in revised form 19 November 2008; accepted 27 November 2008
Available online 14 January 2009

Abstract

From the perspective of high temperature structural applications, it is important to evaluate temperature dependent mechanical properties of titanium diboride (TiB_2) ceramics. The present study reports the effect of $TiSi_2$ content (up to 10 wt.%) and temperature on hardness and strength of TiB_2. The hardness properties were measured from room temperature (RT)—900 °C in vacuum; the four-point flexural strength properties were evaluated at selected temperatures in air up to 1000 °C. An attempt has been made to discuss the difference in hardness and strength properties with sinter-aid amount and microstructure. Our experimental results clearly indicated that the addition of 2.5 wt.% $TiSi_2$ to TiB_2 resulted almost full densification at a lower hot pressing temperature of 1650 °C without compromising on the high temperature strength and hardness properties. The hot pressed TiB_2–2.5 wt.% $TiSi_2$ ceramic could retain moderate strength of more than 400 MPa and hardness of 9 GPa at 1000 °C and 900 °C, respectively.

Keywords: TiB_2; Hot pressing; Hot hardness; High temperature strength

1. Introduction

In the last few decades, ceramics have emerged as a new generation of high temperature materials for aerospace and other structural applications. Transition metal diborides (TiB_2, ZrB_2, HfB_2, etc.) are commonly known as ultra-high temperature ceramics (UHTCs) as they possess melting temperatures greater than 3000 °C.[1] These materials have been considered for high temperature structural applications, such as thermal protection materials for advanced reentry vehicles, furnace elements, molten-metal crucibles and high temperature electrodes in view of their high melting points, superior mechanical properties, oxidation and corrosion resistance.[1–9]

In particular, TiB_2 is attractive for applications such as cutting tools, wear resistant parts, armor material and electrode materials in metal smelting because of its' excellent combination of properties including high hardness, elastic modulus, high strength to weight ratio, wear resistance, good thermal and electrical conductivity. However, the applications of monolithic TiB_2 is rather limited due to the difficulties in obtaining fully dense materials even with an applied pressure at extremely high temperatures (~2000 °C). TiB_2 is difficult to sinter mainly because of its covalent bonding nature, low self-diffusion coefficient and presence of oxide layer (TiO_2 and B_2O_3) on TiB_2 powder surface.[6] Hence, the use of metallic/non-metallic sinter additives is essential to enhance the sinterability of TiB_2.

It has to be mentioned here that although TiB_2 exhibits a unique combination of properties and has potentiality for high temperature applications, very few reports are available on the high temperature mechanical properties of TiB_2 materials. Hot hardness tests have been widely used as a standard tool to evaluate the high temperature mechanical behavior of various ceramics, including borides.[1,9–13] Hardness is one of the most important factors in selecting ceramics for various engineering applications, like abrasive wear, etc. Additionally, the hardness at different temperatures can give a good indication of variation of strength of materials with temperature.[10] Elevated temperature mechanical strength property of some of the advanced ceramic composites is also reported in the published literature.[1,14–27] The high temperature strength properties are very sensitive to microstructural phase assemblage or sinter-additive content. As far as the high temperature proper-

* Corresponding author.
E-mail address: gbraju@iitk.ac.in (G.B. Raju).

0955-2219/$ – see front matter © 2008 Elsevier Ltd. All rights reserved.
doi:10.1016/j.jeurceramsoc.2008.11.018

ties of TiB_2 are concerned, majority of the investigations are limited to monolithic TiB_2. Recently, we have reported the sintering parameter optimization and microstructure development of TiB_2–$TiSi_2$ composites.[28] It is of interest to evaluate the high temperature hardness and strength properties of the developed TiB_2–$TiSi_2$ composites. Such a study would indicate the feasibility of their high temperature application.

2. Experimental procedure

2.1. Processing and microstructural characterization

In the present investigation, TiB_2–$X TiSi_2$ ($X = 0$, 2.5, 5 and 10 wt.% $TiSi_2$) materials were processed from commercially available TiB_2 (Grade F, H.C. Starck GmbH and Co., Goslar, Germany) and $TiSi_2$ (Goodfellow Cambridge Limited, England) powders. The TiB_2 powder had a median particle size (D_{50}) of 0.9 μm and a specific surface area of 2.92 m^2/g. The major impurities in the powders were carbon (0.3 wt.%) and oxygen (1.9 wt.%). The $TiSi_2$ powder (99% purity) was used as a sintering-aid and had D_{50} of 3.5 μm and specific surface area of 0.7 m^2/g. An approximate amount of powder mixtures were hot pressed at a temperature of 1650 °C for 1 h, with an applied pressure of 30 MPa, in a flowing argon atmosphere. Relative density of the samples was measured using the image analysis technique. The crystalline phases in the starting powders, hot pressed and strength tested samples were analyzed using XRD (Rigaku, Japan). The microstructural investigation of the polished and chemically etched surfaces of TiB_2 was performed by means of a scanning electron microscope (SEM) (Quanta FEI 200, Eindhoven, the Netherlands) with attached energy-dispersive spectroscopy (EDS).

The densification data of the hot pressed samples is presented in Table 1. The monolithic TiB_2 could be densified to only 94.4% theoretical density (ρ_{th}) after hot pressing at 1650 °C for 1 h. However, the density of TiB_2 samples increases with $TiSi_2$ sinter additive and the maximum of ~99% ρ_{th} is achievable by adding a small amount of $TiSi_2$ (2.5–10 wt.%), after hot pressing at 1650 °C. In order to compare the properties of the TiB_2 composites, reference monolithic TiB_2 samples were fabricated by hot pressing at 1800 °C for 1 h. It has to be noted here that the in-house processed TiB_2 powders were used for the fabrication of reference monolithic TiB_2, and the major impurities in the powders were oxygen (~0.5 wt.%), carbon (~0.6 wt.%) and nitrogen (~0.6 wt.%). The D_{50} of in-house TiB_2 powders was about 1.2 μm and the specific surface area was 1.49 m^2/g. The reference monolithic TiB_2 exhibited a maximum density of 97.8% ρ_{th} and was characterized by equiaxed grains, having an average grain size of 1.5 μm.

The microstructural analysis shows that hot pressed TiB_2 samples containing up to 5 wt.% $TiSi_2$ consist of TiB_2 and Ti_5Si_3 as major phases, while $TiSi_2$ along with TiB_2 and Ti_5Si_3 are observed for TiB_2–10 wt.% $TiSi_2$. The details of densification mechanism, microstructure, sintering reactions, room temperature (RT) mechanical and electrical properties of the TiB_2–$TiSi_2$ materials were reported elsewhere.[28] A representative microstructure of the TiB_2–10 wt.% $TiSi_2$ composite is presented in Fig. 1a. The microstructure analysis of the TiB_2–10 wt.% $TiSi_2$ composite clearly reveals the presence of three distinct phases. The grey phase, constituting the major area fraction of the micrographs corresponds to TiB_2, while the phase appearing in brightest contrast, located in the intercrystalline regions, corresponds to Ti_5Si_3. The dark contrasting phase ($TiSi_2$) can be observed along the grain boundaries of TiB_2. A closer look at Fig. 1a reveals that the microstructure of the TiB_2 composite consists of bimodal TiB_2 grains (typically a large fraction of the equiaxed grains varying in size from 1.5 μm to 4 μm and some coarser faceted TiB_2 grains varying in size from 4 μm to 7 μm with an aspect ratio of ~2.5). Such characteristic grain morphology is commonly observed for all the TiB_2 samples that were hot pressed at 1650 °C.

From the etched microstructures of different TiB_2 samples, the average grain size of TiB_2 was measured on multiple SEM images using the conventional linear intercept method. The reported grain size values were based upon the measurements of at least 500 grains. The average grain size of the TiB_2 samples is recorded in Table 1. The average grain size of reference monolithic TiB_2 (hot pressed at 1800 °C) is relatively lower than that of the TiB_2 hot pressed at 1650 °C. It indicates that the grain size of TiB_2 in the present study is mainly affected by the type of the starting powders rather than the hot pressing temperature. The average grain size of TiB_2 varied within a narrow range of 2.3–3.6 μm for all the TiB_2–$TiSi_2$ samples that were hot pressed at 1650 °C. However, the finer grain size of 2.3 μm was measured with the TiB_2 containing up to 2.5 wt.% $TiSi_2$. These observations indicate that an optimal amount of $TiSi_2$ addition inhibits the grain growth of TiB_2 during hot pressing. In the literature, it was reported that the anisotropy of the hexag-

Table 1
Densification, average grain size and Vickers hardness (H_v) values at various temperatures of TiB_2–$TiSi_2$ materials hot pressed at 1650 °C for 1 h.

Material composition (in wt.%)	Relative density (% ρ_{th})	Average grain size (μm)	Vickers hardness (GPa)			
			At RT	At 300 °C	At 600 °C	At 900 °C
Monolithic TiB_2 [a]	97.8	1.5 ± 0.2	25.3 ± 1.8	13.9 ± 1.4	10.8 ± 0.7	8.2 ± 0.7
Monolithic TiB_2 [b]	94.4	3.6 ± 0.7	21.2 ± 1.1	13.8 ± 0.4	9.8 ± 0.5	7.2 ± 0.5
TiB_2–2.5$TiSi_2$	98.8	2.3 ± 0.3	27.0 ± 1.7	15.1 ± 0.3	11.5 ± 0.6	8.9 ± 0.3
TiB_2–5.0$TiSi_2$	99.6	3.0 ± 0.6	26.8 ± 1.0	14.1 ± 0.8	10.6 ± 0.6	7.8 ± 0.5
TiB_2–10.0$TiSi_2$	99.6	3.5 ± 0.5	23.7 ± 2.7	13.1 ± 0.9	9.8 ± 0.6	8.0 ± 0.4

[a] Hot pressed at 1800 °C for 1 h.
[b] Hot pressed at 1650 °C for 1 h.

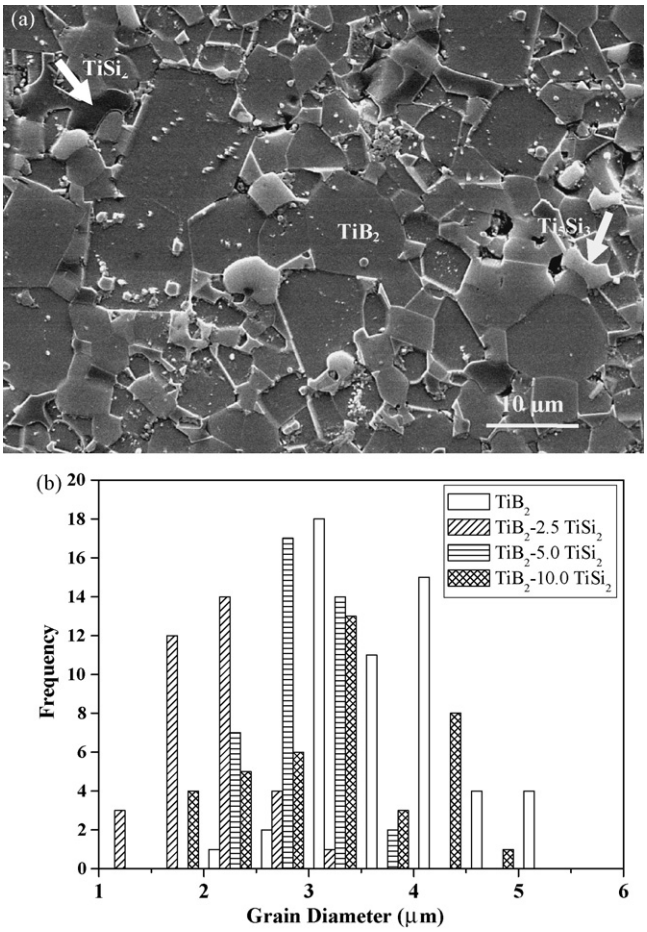

Fig. 1. SEM image of the hot pressed TiB_2–10 wt.% $TiSi_2$ etched surface reveals TiB_2 [grey phase], Ti_5Si_3 [bright phase] and $TiSi_2$ [dark phase] (a) and the histogram shows the effect of $TiSi_2$ sinter additive on TiB_2 grain size (b).

onal crystal structure results in deleterious internal stresses and the onset of spontaneous microcracking during cooling, if grain size of TiB_2 exceeds the critical grain size of 15 μm.[9] In the present study, the average grain size for all the TiB_2 samples (≤3.6 μm) is well below the critical grain size. Fig. 1b shows the grain size distribution of TiB_2 materials and it is evident that $TiSi_2$ addition (up to 2.5 wt.%) refines the grain size of TiB_2. A closer observation of the data presented in Fig. 1b reveals that the mean or peak in the individual grain size distribution shifts toward right as the addition of $TiSi_2$ is increased from 2.5 wt.% to 10 wt.%. The influence of grain size on material properties will be discussed later.

2.2. Hot hardness

The samples (5 mm × 5 mm × 10 mm) for hot hardness measurements were prepared from the hot pressed discs and polished up to 0.25 μm finish with diamond paste and finally polished with γ-Al_2O_3 (0.05 μm). The polished samples were ultrasonically cleaned in acetone for 10 min. The samples were indented using a high temperature hardness tester (QM-2, Nikon, Japan) in a vacuum of less than 5×10^{-3} Pa. The sample was heated to the desired temperature for the experiment; indents were made at RT (23 °C), 300 °C, 600 °C and 900 °C using a load of 9.8 N. The load was maintained for 10 s, and the measured hardness is an average of at least four or five indents that were produced at each test temperature. The indent diagonals were measured in situ at respective temperature with a digital micrometer eyepiece. After the hot hardness tests, the indent diagonal lengths were carefully measured using SEM. We have considered the measurements from SEM images, while calculating hardness values. In the present investigation, irrespective of the test temperature, it was observed that the hardness values calculated by in situ measurements were lower (about 1 GPa) than the SEM measurements. This variation in hardness may be due to the over estimation of diagonal lengths in case of in situ measurements.

2.3. Flexural strength testing

The specimens for strength measurements were cut from the hot pressed disks and machined into bar shapes with dimensions of 3 mm × 4 mm × 40 mm. All the test samples were polished to a surface roughness of $R_a \sim 0.20$ μm by standard ceramographic techniques. The surface roughness of the samples was measured by using a laser surface profilometer. The edges of all the specimens were chamfered, to minimize the effect of stress concentration due to machining flaws. The RT bend tests were performed on a universal testing machine (INSTRON 4465, USA), whereas the high temperature tests (at 500 °C and 1000 °C) were carried out in ambient air using a universal testing machine (INSTRON 8562, England) equipped with a high temperature furnace. For the high temperature strength measurement, the temperature was increased from RT to the test temperature at a heating rate of 15 °C/min, where it was hold for 5 min prior to application of the load. Following the fracture, the sample was furnace cooled by disconnecting the power to the furnace. The flexural strength was measured on a four-point bending configuration using silicon carbide fixture, with a crosshead speed of 0.5 mm/min and inner and outer spans of 10 and 30 mm, respectively. For each ceramic composition, four or five samples were tested for strength measurement. The topography of the fractured surfaces was investigated using SEM.

3. Results

3.1. Hot hardness

The measured hardness values of TiB_2 samples as a function of temperature are presented in Table 1. The standard deviation of reported hardness values was within ±7%. The semilogarithmic hardness of the TiB_2 samples as a function of temperature is plotted in Fig. 2. A common observation is that the hardness of all the materials at any given temperature varies over a narrow window. Among all the samples, TiB_2–2.5 wt.% $TiSi_2$ exhibited a better hardness property and the hardness varied from 27 GPa at RT to 8.9 GPa at 900 °C. At RT, the monolithic TiB_2 (hot pressed at 1800 °C) shows a little lower hardness than the TiB_2 samples containing up to 5 wt.% $TiSi_2$. However, it is interesting to note that the hardness of the monolithic TiB_2 is compara-

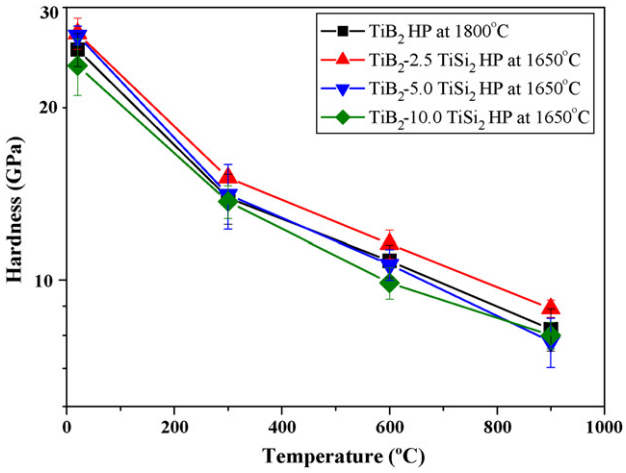

Fig. 2. A semilogarithmic representation of the hardness of TiB_2 samples [after hot pressing (HP) at 1650 °C and 1800 °C, for 1 h] as a function of temperature.

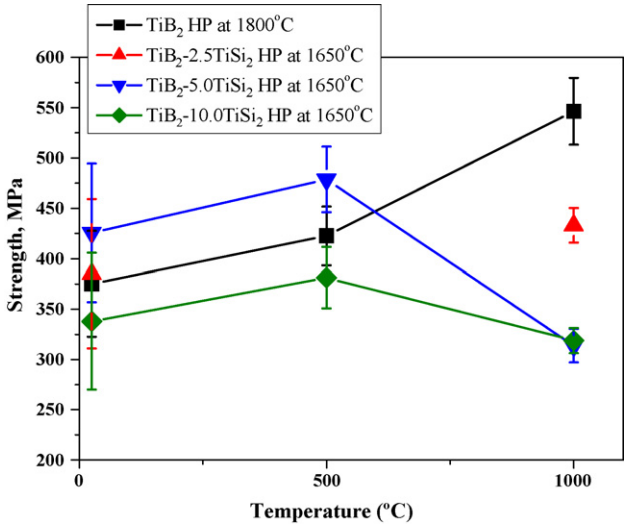

Fig. 3. Effect of temperature on the four-point flexural strength of TiB_2 samples after hot pressing (HP) at 1650 °C and 1800 °C for 1 h, relative to the amount of $TiSi_2$.

ble with the other TiB_2 samples (containing ≥5 wt.% $TiSi_2$) at elevated temperatures. For example, the hardness of monolithic TiB_2 and TiB_2–5 wt.% $TiSi_2$ is measured to be 8.2 GPa and 7.8 GPa, respectively at 900 °C.

3.2. Flexural strength

In Fig. 3, the effect of temperature on flexural strength of the hot pressed TiB_2–$TiSi_2$ samples is presented. Among all the compositions, TiB_2–5 wt.% $TiSi_2$ showed the highest RT strength (~426 MPa). This can be attributed to its high density (see Table 1). The increased amount of second phase is observed to reduce the RT strength (~337 MPa) of TiB_2–10 wt.% $TiSi_2$. Up to 500 °C, the fracture strength is observed to increase for all the TiB_2 compositions that were densified to more than 97% ρ_{th}. Both the reference monolithic TiB_2 and TiB_2–2.5 wt.% $TiSi_2$ specimens could retain flexural strength of more than 400 MPa up to 1000 °C, whereas the flexural strength of the other monolithic TiB_2 (hot pressed at 1650 °C) and TiB_2 specimens containing either 5 wt.% or more $TiSi_2$ decreased with increasing the temperature. However, a minimum of 79% RT strength could be retained for all TiB_2–$TiSi_2$ compositions. For the strength tested samples, the standard deviation was varied over a range within ±4–24%. It is interesting to note that variation in strength values decreased systematically with the temperature. However, in all the cases the maximum deviation is observed with monolithic TiB_2 (hot pressed at 1650 °C), owing to its poor densification (see Table 2).

3.3. Fractography

The crystalline phases of TiB_2 samples that are detected by XRD after the flexural strength tests at various temperatures are shown in Table 2. The crystalline phases of each TiB_2 specimen remain the same up to 500 °C. But the samples which were tested at 1000 °C consist only of crystalline TiO_2 (rutile) and TiB_2 phases. Fig. 4 shows a representative XRD pattern of monolithic TiB_2 and TiB_2–5 wt.% $TiSi_2$. The effect of temperature on the microstructure/crystalline phases of the TiB_2–5 wt.% $TiSi_2$ composite can be clearly seen from Fig. 4. Although TiB_2 is the major phase for the TiB_2–5 wt.% $TiSi_2$ at RT, increasing the temperature to 1000 °C resulted TiO_2 becoming the predominant phase. At 1000 °C, both the TiB_2 samples irrespective of their composition contain only TiO_2 and TiB_2 as main constituent phases and such observations indicate the oxidation of the samples (see Fig. 4). Representative SEM images of fracture surfaces are shown in Fig. 5, and the characteristics of inter/transgranular fracture is distinguished in each image at some representative

Table 2
High temperature flexural strength values of the TiB_2–$TiSi_2$ materials hot pressed at 1650 °C for 1 h. XRD crystalline phases of the samples at room temperature (RT), 500 °C and 1000 °C after the flexure test can also be noted.

Material composition (in wt.%)	Four-point flexural strength (MPa)			Crystalline phases		
	At RT	At 500 °C	At 1000 °C	At RT	At 500 °C	At 1000 °C
Monolithic TiB_2 [a]	375.1 ± 52.5	422.5 ± 29.1	546.1 ± 33.2	TiB_2	TiB_2	TiB_2, TiO_2
Monolithic TiB_2 [b]	365.0 ± 88.5	287.4 ± 44.4	267.8 ± 43.4	TiB_2	TiB_2	TiB_2, TiO_2
TiB_2–2.5$TiSi_2$	380.9 ± 74.0	–	433.0 ± 17.3	TiB_2, Ti_5Si_3	–	TiB_2, TiO_2
TiB_2–5.0$TiSi_2$	425.7 ± 68.8	478.6 ± 32.6	313.7 ± 16.6	TiB_2, Ti_5Si_3	TiB_2, Ti_5Si_3	TiB_2, TiO_2
TiB_2–10.0$TiSi_2$	337.9 ± 67.9	381.1 ± 30.4	318.8 ± 12.5	TiB_2, Ti_5Si_3, $TiSi_2$	TiB_2, Ti_5Si_3, $TiSi_2$	TiB_2, TiO_2

[a] Hot pressed at 1800 °C for 1 h.
[b] Hot pressed at 1650 °C for 1 h.

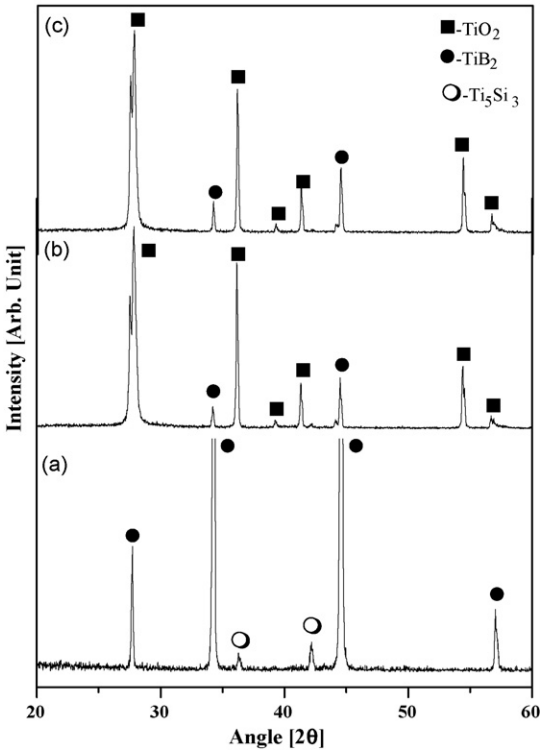

Fig. 4. XRD patterns of the hot pressed TiB_2–5 wt.% $TiSi_2$ specimen after four-point bend test at RT [pattern (a)], at 1000 °C [pattern (b)] and reference monolithic TiB_2 after the bend test at 1000 °C [pattern (c)].

locations. At RT, cleavage fracture is the dominant fracture mode with the reference monolithic TiB_2, hot pressed at 1800 °C, while the fracture occurred mainly by mixed (intergranular and cleavage) pattern for all the TiB_2–$TiSi_2$ samples hot pressed at 1650 °C. Fig. 6 illustrates the topography of the strength tested samples (at 500 °C) and the sample surfaces do not show any indication of oxidation. Both the reference monolithic TiB_2 and the other monolithic TiB_2 hot pressed at 1650 °C fractured predominantly via mixed mode of fracture. Intergranular fracture is the dominant fracture mode for the TiB_2 reinforced with $TiSi_2$. At 1000 °C, the fracture surfaces of all the samples reveal the evidence of oxidized microstructure, presence of cavitations (due to the grain pull outs) and microcracks (see Fig. 7). The EDS analysis of fracture surfaces of all the TiB_2 samples irrespective of their composition shows the presence of Ti, B and O. A representative EDS spectrum is shown for TiB_2–2.5 wt.% $TiSi_2$ as an inset in Fig. 7b.

4. Discussion

The high temperature strength and hardness properties of the TiB_2 materials will now be analyzed in terms of the following factors: (a) sinter density, (b) TiB_2 grain size and (c) sinter additive ($TiSi_2$) content.

4.1. Temperature dependent hardness

It is known that the brittle materials can be plastically deformed even at temperatures below $0.5T_{mp}$ (melting temperature) under the application of a large hydrostatic stress field component.[10] The RT hardness of the monolithic TiB_2 and TiB_2–$TiSi_2$ samples is measured to vary from 21 GPa to 27 GPa (see Table 1). Such a variation in the hardness of the samples can be attributed to the densification and amount of sinter additive. The less densified monolithic TiB_2 (hot pressed at 1650 °C) exhibits the lowest hardness of 21 GPa, while the hardness of the reference monolithic TiB_2 is 25 GPa. The hardness of the TiB_2 composites increased with the $TiSi_2$ (up to 5 wt.% $TiSi_2$) addition and further increasing the $TiSi_2$ content to 10 wt.% resulted in lower hardness (24 GPa) of TiB_2 despite its full densification (99.6% ρ_{th}). From the above observations, it can be realized that although the TiB_2 composites consist relatively softer phases like $TiSi_2$ (8.7 GPa) and Ti_5Si_3 (9.8 GPa),[29] the addition of small amount of $TiSi_2$ ($\leq$5 wt.%) does not degrade the hardness of TiB_2. The hardness values of TiB_2–2.5 wt.% $TiSi_2$ composite is relatively higher, when compared with other TiB_2 samples. The improvement in hardness is mainly because of its higher density and less amount of secondary phase. Although, the TiB_2–2.5 wt.% $TiSi_2$ exhibited maximum hardness of ~27 GPa at RT, a steep fall in hardness is observable at 300 °C (Fig. 2). Similar behavior was also noticed with the other TiB_2 samples as well. A common observation is that the hardness of all the TiB_2 samples decreases with increase in the temperature. The decrease in hardness of TiB_2–$TiSi_2$ materials reflects that the indentation plasticity causes softening of the materials at high temperatures.

It can be further mentioned here that Munro[9] reported the hardness of monolithic TiB_2 (the average grain size of TiB_2 ~ 9 μm) varied between 25.0 GPa and 4.6 GPa over a range of temperature from RT to 1000 °C. In another work, Jungling et al.[30] observed that hot hardness of TiB_2-hard metals varied between 7.3 GPa (for TiB_2–5 vol.% Fe–Fe_2B binder) and 4.8 GPa (for TiB_2–20 vol.% Fe–Cr–Ni–Fe_2B binder) at 800 °C. Therefore, a comparison with the reported values reveals that our newly developed TiB_2–$TiSi_2$ materials can retain higher hardness (7–9 GPa) at high temperature (900 °C) and it can be attributed to the finer grain size.

4.2. Temperature dependent flexural strength

Fig. 3 shows the effect of temperature on bend strength of TiB_2–$TiSi_2$ composites. It can be realized the strength increases (from 375 MPa at RT to 546 MPa at 1000 °C) with temperature for the reference TiB_2. Munro[9] as well as Baumgartner and Steiger[31] reported an increase in strength with increase in temperature (up to 1500 °C) for monolithic TiB_2. They attributed this to the relief of internal stresses, which arise from the anisotropic thermal expansion of the microcrystalline constituent particles and crack healing due to oxidation (i.e. the formation of B_2O_3 up to about 1000 °C) as well. However, the latter may not be true, since the RT strength of TiB_2 specimens, oxidized at higher temperatures, appears to be diminished by oxidation.[32,33] Hence, we believe that relief of the internal stresses in TiB_2 at higher temperatures would enhance the flexural strength of TiB_2. The present study revealed an interesting and new observation of decrease in strength with temperature

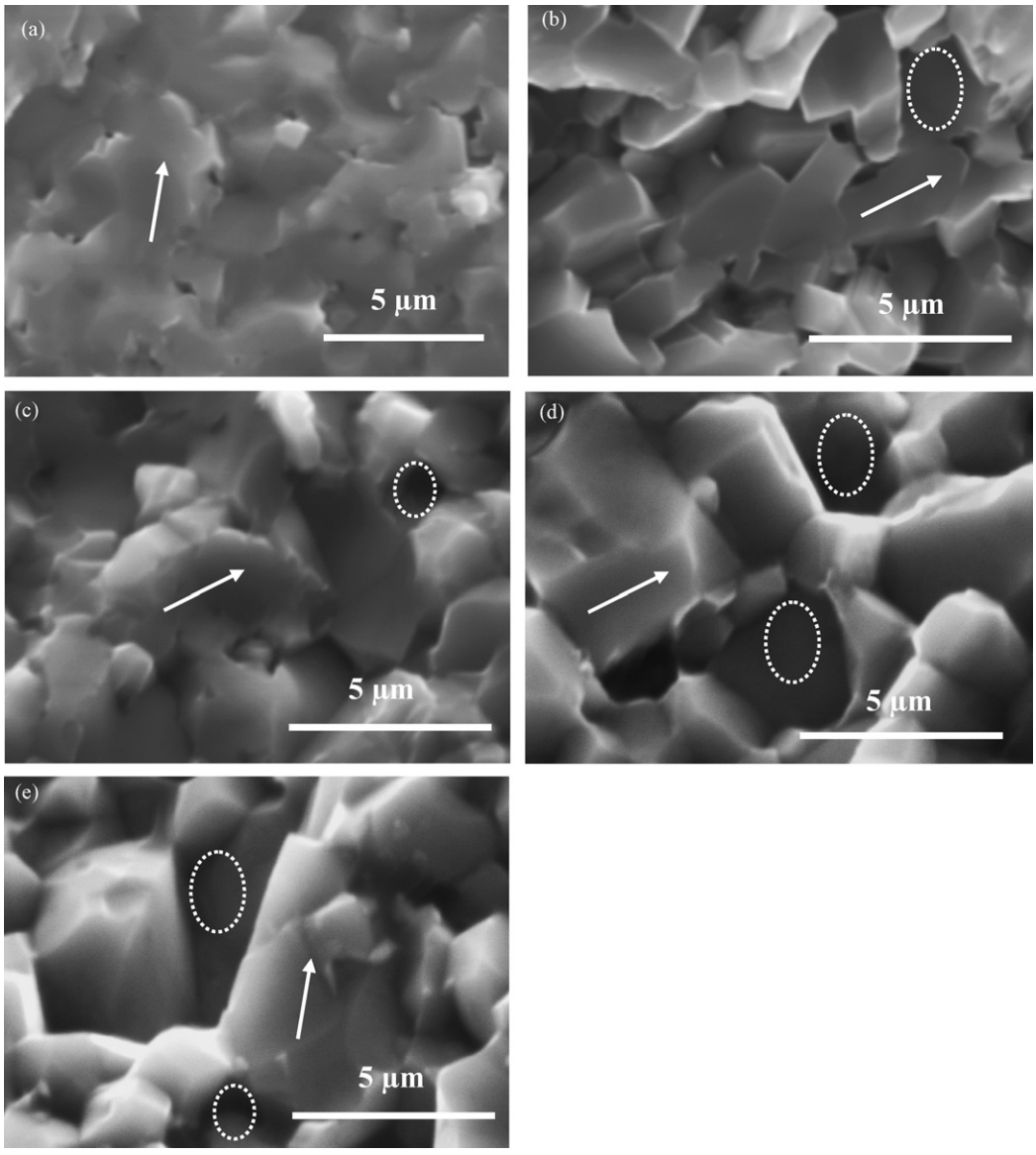

Fig. 5. Fracture surfaces of the hot pressed reference monolithic TiB_2 [hot pressed at 1800 °C] shows that fracture occurred predominantly via cleavage fracture mode (a). The other monolithic TiB_2 (b), TiB_2–2.5 wt.% $TiSi_2$ (c), TiB_2–5 wt.% $TiSi_2$ (d), and TiB_2–10 wt.% $TiSi_2$ (e) [hot pressed at 1650 °C] shows the mixed mode of intergranular and transgranular fracture at RT. The single headed arrow illustrates the cleavage mode of fracture and the encircled regions correspond to intergranular fracture.

for the monolithic TiB_2 samples, hot pressed at 1650 °C (see Table 2). Poor densification (~94% of ρ_{th}) and thereby the presence of large porosity as well as the cavitations and microcracks, in combination, should have caused the fracture of TiB_2 at low loads at or above 500 °C (see Figs. 6b and 7a). It is quite possible that the presence of pores leads to initiation of cracks and degrades the strength.

Up to 500 °C, TiB_2–5 wt.% $TiSi_2$ exhibited maximum strength among all the compositions. Fig. 5c shows that at RT, the fracture occurs via mixed mode of fracture with the TiB_2–5 wt.% $TiSi_2$ composite. If we look closely at Fig. 6c, the fracture of the TiB_2–5 wt.% composite takes place predominantly by intergranular fracture at 500 °C. Better density and the change in the mode of fracture from cleavage to intergranular fracture might have improved the fracture resistance at 500 °C. However, at 1000 °C, the degradation in strength is noticeable for the monolithic TiB_2 (HP at 1650 °C) and TiB_2 composites (containing ≥5 wt.% $TiSi_2$) excluding the reference monolithic TiB_2 and the TiB_2–2.5 wt.% $TiSi_2$. The decrease in strength can be attributed to grain pullouts and microcracking of the materials. Fig. 7b reveals the minimal presence of such characteristic features in case of the TiB_2–2.5 wt.% $TiSi_2$.

At 1000 °C, the flexural strength of reference monolithic TiB_2 is relatively higher than all the TiB_2–$TiSi_2$ compositions. It implies that at elevated temperature the grain boundary sliding at the boundary of TiB_2/Ti_5Si_3 and TiB_2/$TiSi_2$ grains result in fracture at low loads for the TiB_2 composites. Since the brittle to ductile transition temperature of $TiSi_2$ is 800 °C and lies in the range of 1000–1200 °C for Ti_5Si_3, these phases are expected to exhibit plasticity at or above 800 °C with the application of

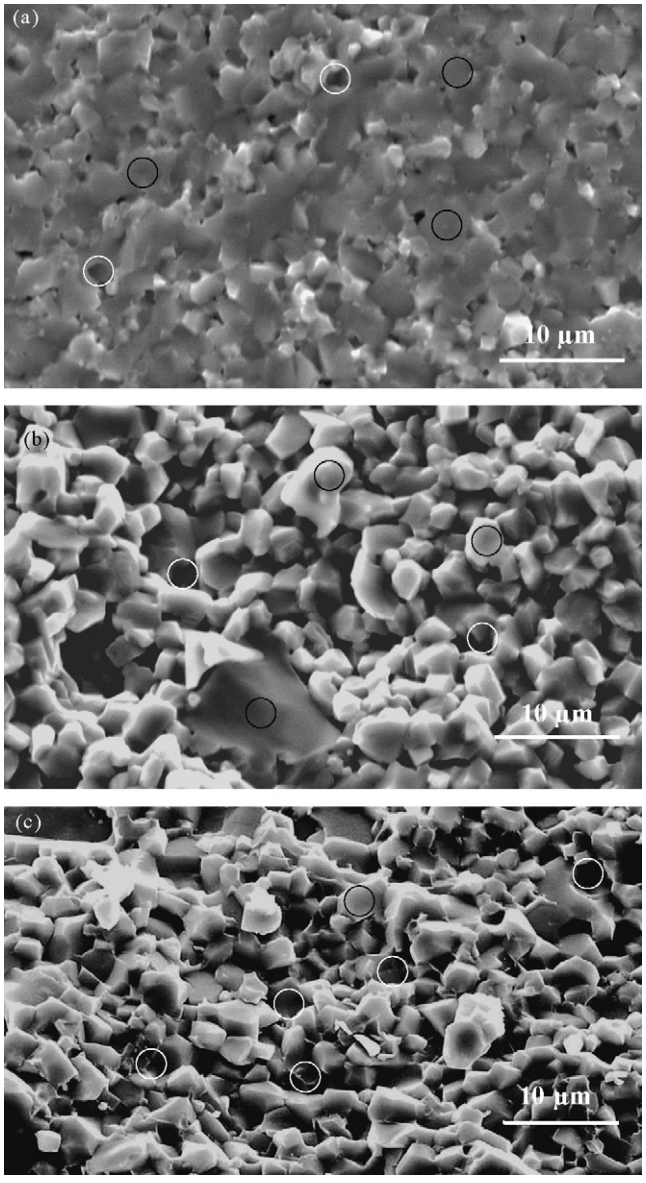

Fig. 6. Fracture surfaces of the reference monolithic TiB_2 [hot pressed at 1800 °C] (a) and the other less densified monolithic TiB_2 [hot pressed at 1650 °C] (b) both exhibits mixed mode of fracture at 500 °C. However, the latter shows additionally cavitations and microcracks (b). TiB_2–5 wt.% $TiSi_2$ reveals the fracture is predominantly of intergranular nature at 500 °C (c). The regions encircled with black circle illustrate the transgranular fracture and the white circles indicate intergranular fracture.

load.[34–38] Hence, the plastic deformation of $TiSi_2$ and Ti_5Si_3 at high temperature may also contribute to the strength degradation in the TiB_2 composites. In the present study, though all the strength tested samples experienced oxidation during the flexural strength testing at 1000 °C, both the reference monolithic TiB_2 and TiB_2–2.5 wt.% $TiSi_2$ composite retained the RT strength despite oxidation. On the contrary, all the other samples showed a decrease in strength. Hence, it can be inferred that at high temperatures, the strength of monolithic TiB_2 is mainly influenced by densification; while, both the sinter density and sinter additive amount determines the strength of TiB_2 composites.

Table 3
Summary of research results illustrating the effect of temperature on flexural strength of some important high temperature ceramics [HP: hot pressing, PS: pressureless sintering, SPS: spark plasma sintering, four-P: four-point and three-P: three-point flexural strength].

Material composition (in wt.%)	Processing details	Relative density (% (th)	Bend test conditions	Flexural strength (MPa)							Reference
				RT	500 °C	800 °C	1000 °C	1200 °C	1400 °C	1500 °C	
TiB_2	PS, 1900 °C, 1 h	>95	Three-point, argon	310	–	–	370	405	–	–	31
TiB_2	PS, 2100 °C, 1 h	99.3	Three-point, argon	290	305	–	390	400	–	–	31
TiB_2	–	99.5	Three-point	400	429	–	459	471	–	489	9
ZrB_2	HP, 1900 °C, 30 min	86.5	Four-point, air	351	–	342	317	312	219	–	20
ZrB_2–4Ni	HP, 1850 °C, 30 min	98	Four-point, air	371	–	624	237	–	–	–	20
HfB_2–22.1 vol.% SiC–5.9 vol.% HfC	HP, 1900 °C	–	Four-point, air	770	–	–	–	–	–	310	2
85.6βSiC–0.9αSiC–2.9AlN–10.6Y_2O_3	HP, 1900 °C, 1 h	98.1	Four-point, nitrogen	650	–	–	–	–	630	550	24
87.49Si_3N_4–1.68Lu_2O_3	HP, 1950 °C, 1 h	98.5	Four-point, nitrogen	800	–	–	–	750	600	–	21
$MoSi_2$	SPS, 1300 °C, 1 h	98.2	Three-point	550	–	420	325	–	–	–	25
Al_4SiC_4	Reaction HP, 1950 °C, 1 h	95.4	Three-point, air	297	–	–	385	388	–	–	27

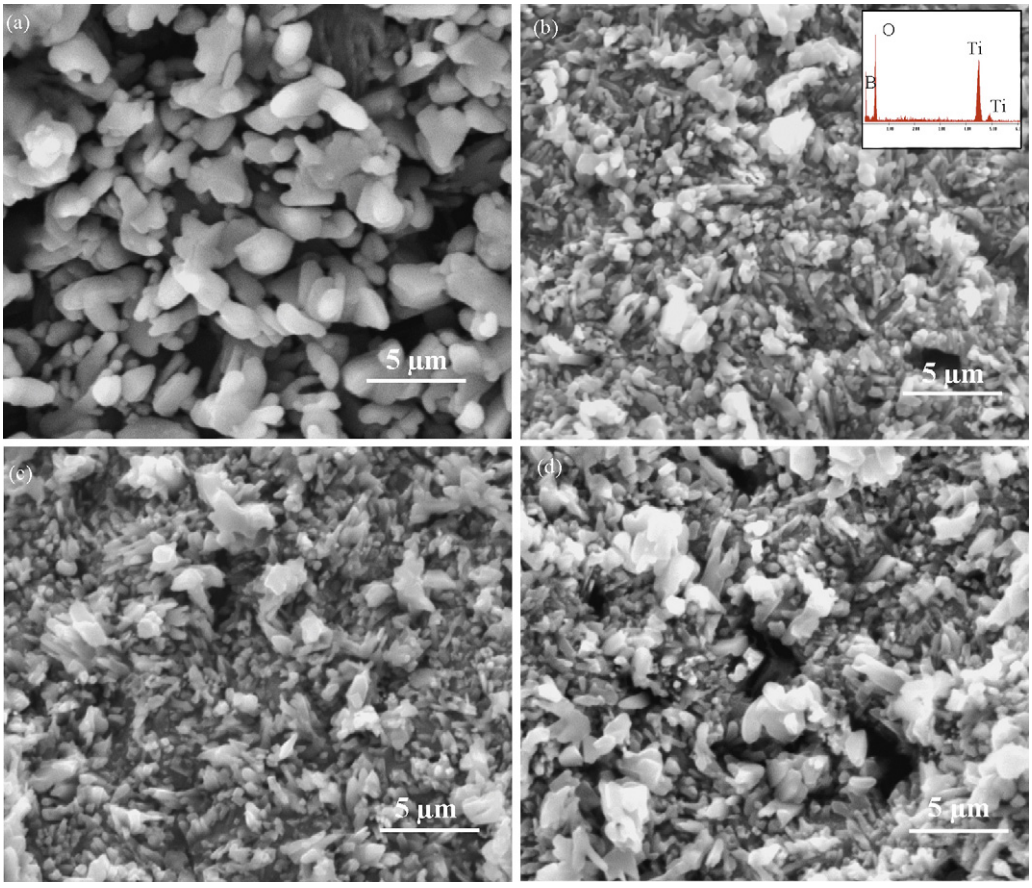

Fig. 7. Fracture surfaces of the hot pressed monolithic TiB_2 (a), TiB_2–2.5 wt.% $TiSi_2$ (b), TiB_2–5 wt.% $TiSi_2$ (c) and TiB_2–10 wt.% $TiSi_2$ (d) at 1000 °C. Note the evidence of oxidized surface of fractured samples in (a)–(d). The EDS analysis of fracture surfaces of all the TiB_2 samples shows the presence of Ti, B and O and a representative EDS spectrum is shown for TiB_2–2.5 wt.% $TiSi_2$ as an inset.

A summary of research results illustrating the effect of temperature on flexural strength of some of the important high temperature structural ceramics is presented in Table 3. It can be observed that for both the monolithic TiB_2 and Al_4SiC_4 ceramics, strength increases with temperature up to 1200 °C. In fact, TiB_2 could retain the strength up to 1500 °C. In case of ZrB_2-based materials, degradation in strength is noticeable at or above 1000 °C. A common observation is that SiC and Si_3N_4 ceramics exhibit high values of strength at both the room and high temperatures, when compared with TiB_2 and all the other ceramics (see Table 3). Although SiC and Si_3N_4 composites exhibited better strength properties (varying in the range of 550–750 MPa up to 1500 °C), a trend of decrease in strength with temperature is evident. A closer look at Tables 1–3 reveals that the newly developed TiB_2 materials are densified relatively at low processing temperatures (reference monolithic TiB_2 at 1800 °C and TiB_2–$TiSi_2$ composites at 1650 °C for 1 h), when compared with the other high temperature ceramics excluding the $MoSi_2$. It also can be noted here that all the densified TiB_2–$TiSi_2$ samples (except monolithic TiB_2 hot pressed at 1650 °C) are measured with more than 300 MPa at 1000 °C and the strength values are comparable with many of the structural ceramics with the exception of the SiC and Si_3N_4. In contrast, the densification of SiC requires much higher hot pressing temperature (>1800 °C). Also, Si_3N_4-based ceramics require high sintering temperatures and its microstructure is very sensitive to the sinter-aid additions. In this perspective, densification of TiB_2–$TiSi_2$ ceramics is possible at low sintering temperatures with finer grain size. In one of our earlier studies, it was reported that the TiB_2–$TiSi_2$ materials possessed low electrical resistivity (10–12.6 μΩ cm) and was only six times higher than that of copper.[28] Such better electrical properties of TiB_2 would enable the samples to be machined into required near net shapes using electric discharge machining. From the above discussion, it can be inferred that TiB_2–$TiSi_2$ materials could be a better choice for high temperature applications up to 1000 °C, in view of their low processing temperatures with better combination of hardness and strength properties.

Finally, the present experimental results clearly confirm the advantage of using $TiSi_2$ as a sintering-aid to improve densification as well as to retain high temperature strength and hardness properties. For monolithic TiB_2 materials to retain strength at high temperature, high densification (>97% ρ_{th}) is essential. But to achieve such high density with monolithic TiB_2, high hot pressing temperature of 1800 °C is needed. We could achieve maximum density of 99% ρ_{th} at a lower hot pressing temperature of 1650 °C with the use of $TiSi_2$ as a sintering aid. However, in the case of composites, retention of strength at high temperature is only possible with better density and minimal amount of sinter additive. Among all the compositions, TiB_2–2.5 wt.%

$TiSi_2$ composite exhibited the best hardness and strength values at high temperatures.

5. Conclusions

The hardness measurements of TiB_2–$TiSi_2$ composites at various temperatures (up to 900 °C) reveal the systematic decrease in the hardness values with the temperature. Among all the compositions, TiB_2–2.5 wt.% $TiSi_2$ exhibited better hardness properties (27 GPa at RT and 9 GPa at 900 °C) due to its higher sinter density and minimal amount of second phase.

Both at RT and 500 °C, the strength increases with $TiSi_2$ content and goes through a maximum at 5 wt.% $TiSi_2$. Broadly, higher strength value is measured at 500 °C than at RT, irrespective of ceramic composition, except the monolithic TiB_2 that is hot pressed at 1650 °C. At RT, all the materials (except the reference monolithic TiB_2) fractured predominantly by inter and transgranular pattern. Among the investigated material compositions, TiB_2–5 wt.% $TiSi_2$ exhibited better strength (∼479 MPa) properties due to its high sinter density and intergranular mode of fracture at 500 °C.

At 1000 °C, the strength values decreased for all the samples except the reference monolithic TiB_2 (hot pressed at 1800 °C) and TiB_2–2.5 wt.% $TiSi_2$. However, the flexural strength of around 314 MPa can be retained in other TiB_2–$TiSi_2$ composites. The decrease in flexural strength values of TiB_2 composites at 1000 °C can be attributed to grain pullouts and microcracking, while all the materials fractured mainly via intergranular mode of fracture.

Acknowledgements

The authors thank Mr. K. Yoon for the help in carrying out the high temperature flexural strength tests at the Korea Research Institute of Standards and Science (KRISS), Korea. G.B. Raju wishes to express sincere gratitude to Dr. M.C. Chu and Dr. B. Phanigrahi for the cooperation in the hot pressing experiments during his brief stay at KRISS.

References

1. Cutler, R. A., *Engineering Materials Handbook, Ceramics and Glasses*, *vol. 4*. ASM International, Metals Park, OH, USA, 1991, p. 787–811.
2. Monteverde, F., Progress in the fabrication of ultra high temperature ceramics: in situ synthesis, microstructure and properties of a reactive hot-pressed HfB_2–SiC composite. *Compos. Sci. Technol.*, 2005, **65**, 1869–1879.
3. Upadhya, K., Yang, J. M. and Hoffman, W. P., Materials for ultrahigh temperature structural applications. *Am. Ceram. Soc. Bull.*, 1997, **58**(12), 51–56.
4. Wiley, D. E., Manning, W. R. and Hunter Jr., O., Elastic properties of polycrystalline TiB_2, ZrB_2 and HfB_2 from room temperature to 1300 K. *J. Less-Common Met.*, 1969, **18**, 149–157.
5. Chamberlain, A. L., Fahrenholtz, W. G., Hilmas, G. E. and Ellerby, D. T., High-strength zirconium diboride-based ceramics. *J. Am. Ceram. Soc.*, 2004, **87**(6), 1170–1172.
6. Basu, B., Raju, G. B. and Suri, A. K., Processing and properties of monolithic TiB_2-based materials. *Int. Mater. Rev.*, 2006, **51**(6), 352–374.
7. Ramberg, J. R., Wolfe, C. F. and Williams, W. S., Resistance of titanium diboride to high-temperature plastic yielding. *J. Am. Ceram. Soc.*, 1985, **68**(3), C-78–C-79.
8. Ramberg, J. R. and Williams, W. S., High temperature deformation of titanium diboride. *J. Mater. Sci.*, 1987, **22**, 1815–1826.
9. Munro, R. G., Material properties of titanium diboride. *J. Res. Natl. Inst. Stand. Technol.*, 2000, **105**(5), 709–720.
10. Wang, H. L. and Hon, M. H., Temperature dependence of ceramics hardness. *Ceram. Int.*, 1999, **25**, 267–271.
11. Koester, R. D. and Moak, D. P., Hot hardness of selected borides, oxides and carbides to 1900 °C. *J. Am. Ceram. Soc.*, 1967, **50**(6), 290–296.
12. Sanders, W. A. and Probst, H. B., Hardness of five borides at 1625 °C. *J. Am. Ceram. Soc.*, 1966, **49**(4), 231–232.
13. Nakano, K., Matsubara, H. and Imura, T., High temperature hardness of titanium diboride single crystal. *Jpn. J. Appl. Phys.*, 1974, **13**(6), 1005–1006.
14. Maloy, S., Heuer, A. H., Lewandowski, J. and Petrovic, J., Carbon additions to molybdenum disilicide: improved high-temperature mechanical properties. *J. Am. Ceram. Soc.*, 1991, **74**(10), 2704–2706.
15. Zhong, X. and Zao, H., High temperature properties of refractory composites. *Am. Ceram. Soc. Bull.*, 1999, **60**, 98–101.
16. Pierce, L. A., Mieskowski, D. M. and Sanders, W., Effect of grain-boundary crystallization on the high-temperature strength of silicon nitride. *J. Mater. Sci.*, 1986, **21**, 1345–1348.
17. Keppeler, M., Reichert, H. G., Broadley, J. M., Thurn, G., Wiedmann, I. and Aldinger, F., High-temperature mechanical behavior of liquid-phase-sintered silicon carbide. *J. Eur. Ceram. Soc.*, 1998, **18**, 521–526.
18. Chen, D., Sixta, M. E., Zhang, X. F., De Jonghe, L. C. and Ritchie, R. O., Role of the grain-boundary phase on the elevated temperature strength, toughness, fatigue, and creep resistance of silicon carbide sintered with Al, B, and C. *Acta Mater.*, 2000, **48**, 4599–4608.
19. Rixecker, G., Wiedmann, I., Rosinus, A. and Aldinger, F., High-temperature effects in the fracture mechanical behavior of silicon carbide liquid-phase sintered with AlN–Y_2O_3 additives. *J. Eur. Ceram. Soc.*, 2001, **21**, 1013–1019.
20. Melendez-Martinez, J. J., Dominguez-Rodriguez, A., Monteverde, F., Melandri, C. and de Portu, G., Characterization and high temperature mechanical properties of zirconium boride-based materials. *J. Eur. Ceram. Soc.*, 2002, **22**, 2543–2549.
21. Guo, S., Hirosaki, N., Yamamoto, Y., Nishimura, T. and Mitomo, M., Improvement of high-temperature strength of hot-press sintering silicon nitride with Lu_2O_3 addition. *Scripta Mater.*, 2001, **45**, 74–86.
22. Park, D. S., Hahn, B. D., Bae, B. C. and Park, C., Improved high-temperature strength of silicon nitride toughened with aligned whisker seeds. *J. Am. Ceram. Soc.*, 2005, **88**(2), 383–389.
23. Zhu, Q. and Shobu, K., High-temperature mechanical properties of SiC–$Mo_5(Si, Al)_3C$ composites. *J. Am. Ceram. Soc.*, 2001, **84**(2), 413–419.
24. Kim, Y. W., Mitomo, M. and Nishimura, T., High-temperature strength of liquid-phase-sintered SiC with AlN and Re_2O_3 (Re = Y, Yb). *J. Am. Ceram. Soc.*, 2002, **85**(4), 1007–1009.
25. Shimizu, H., Yoshinaka, M., Hirota, K. and Yamaguchi, O., Fabrication and mechanical properties of monolithic $MoSi_2$ by spark plasma sintering. *Mater. Res. Bull.*, 2002, **37**, 1557–1563.
26. Song, G. M., Wang, Y. J. and Zhou, Y., Thermomechanical properties of TiC particle-reinforced tungsten composites for high temperature applications. *Int. J. Refract. Met. Hard Mater.*, 2003, **21**, 1–12.
27. Wen, G. W. and Huang, X. X., Increased high temperature strength and oxidation resistance of Al_4SiC_4 ceramics. *J. Eur. Ceram. Soc.*, 2006, **26**, 1281–1286.
28. Raju, G. B. and Basu, B., Densification, sintering reactions and properties of titanium diboride with titanium disilicide as a sintering aid. *J. Am. Ceram. Soc.*, 2007, **90**(11), 3415–3423.
29. Berg, G., Friedrich, C., Broszeit, E. and Berger, C., *Data Collection of Properties of Hard Materials, in Handbook of Ceramic Hard Materials*, *vol. 2*, ed. R. Riedel. WILEY-VCH Verlag GmbH, D-69469 Weinheim (Federal Republic of Germany), 2000, pp. 965–990.
30. Jungling, Th., Sigl, L. S., Oberacker, R., Thummler, F. and Schwetz, K. A., New hardmetals based on TiB_2. *Int. J. Refract. Met. Hard Mater.*, 1993-1994, **12**, 71–88.
31. Baumgartner, H. R. and Steiger, R. A., Sintering and properties of titanium diboride powder synthesized in a plasma-arc heater. *J. Am. Ceram. Soc.*, 1984, **67**(3), 207–212.

32. Koh, Y. H., Kim, H. W. and Kim, H. E., Improvement in oxidation resistance of TiB_2 by formation of protective SiO_2 layer on surface. *J. Mater. Res.*, 2001, **16**(1), 132–137.
33. Matsushita, J., Suzuki, T. and Sano, A., High temperature strength of TiB_2 ceramics. *J. Ceram. Soc. Jpn.*, 1993, **101**, 1074–1077.
34. Mitra, R., Mechanical behavior and oxidation resistance of structural silicides. *Int. Mater. Rev.*, 2006, **51**(1), 13–64.
35. Inui, H., Moriwaki, M., Okamoto, N. and Yamaguchi, M., Plastic deformation of single crystals of $TiSi_2$ with the C54 structure. *Acta Mater.*, 2003, **51**, 1409–1420.
36. Li, J., Jiang, D. and Tan, S., Microstructure and mechanical properties of in situ produced SiC/$TiSi_2$ nanocomposites. *J. Eur. Ceram. Soc.*, 2000, **20**, 227–233.
37. Li, J., Jiang, D. and Tan, S., Microstructure and mechanical properties of in situ produced Ti_5Si_3/TiC nanocomposites. *J. Eur. Ceram. Soc.*, 2002, **22**, 551–558.
38. Rosenkranz, R. and Frommeyer, G., Microstructures and properties of high melting point intermetallic Ti_5Si_3 and $TiSi_2$ compounds. *Mater. Sci. Eng. A*, 1992, **152**, 288–294.